New Proton-Exchange Membrane (PEM)
Based on the Modification of Sulfonated Polystyrene
with MIL-53(Al)-NH₂ for Direct-Methanol Fuel Cell

Salehi, Masoumeh; Karimipour, Gholamreza [*+]***; Montazerozohori, Morteza; Ghaedi, Mehrorang***
Department of Chemistry, Yasouj University, Yasouj, I.R. IRAN

Valiollah Mandanipour [*+]
Department of Applied Chemistry, University of Gonabad, Gonabad, I.R. IRAN

ABSTRACT: *In this study, modified sulfonated polystyrene (SPS) was used as a base for membrane fabrication in Direct Methanol Fuel Cells (DMFCs). The sulfonated polystyrene (SPS) was prepared using ethylsulfate and polystyrene with sulfate attached to the para-position of some phenyl groups in polystyrene backbone and conducted by polyethylene (PE) and different amounts of MIL-53(Al)-NH₂ as metal-organic material, to obtain SPS-PE-MIL-53 as a novel proton-exchange membrane. The membranes were characterized using FT-IR spectroscopy, SEM, and TGA analysis. The proton conductivity, water uptake, oxidative resistance, ionic conductivity, and methanol permeability of the membranes were examined to assess their performance in a direct methanol fuel cell. The modified membrane containing 1% wt SPS, 1% wt PE, and 0.25% wt MIL-53 showed relatively better performance than the other prepared membranes with the selectivity factor of $7.17 \times 10^4 \, S.s/cm^3$ and a maximum peak power density of $17.04 \, mW/cm^2$ with a maximum current density of $115.38 \, mA/cm^2$.*

KEYWORDS: *Sulfonated polystyrene; MIL-53(Al)-NH₂; Proton-exchange membrane; Metal-organic material; Direct methanol fuel cell (DMFC).*

INTRODUCTION

Fuel cells are an emerging technology that offers a brighter future for developing global energy sources with environmental and economic advantages. The fuel cell is a promising source of electrochemical energy that can provide the currently required energy by directly converting a fuel's chemical energy to electrical energy [1-3]. High energy efficiency, high energy density, low noise, almost emission-free, and short-term charging are the advantages of this efficient and clean energy source which could lead to the use of this energy to generate electricity [4-7]. Due to their advantages in using low-cost raw materials, high energy conversion efficiency, and low operating temperatures, Direct Methanol Fuel Cells (DMFCs) have received more attention than other fuel cells [8-11]. DMFC's efficiency depends on the electrolyte membrane. Also, the proton-exchange membrane (PEM) plays the role of a separator between the anode and the cathode. It also facilitates the transfer of protons. PEM has some important advantages,

including the high thermal, mechanical, and chemical resistance, besides preventing fuel passage during fuel cell operation [12]. DMFCs use regenerative methanol as fuel. One of the significant barriers to the broad commercial use of DMFCs on a large scale is methanol crossover. Methanol penetration from the anode to the cathode using the polymer electrolyte membrane can severely degrade the activity of the cathode catalyst, which limits the use of PEMs in DMFCs [13-15]. Given the above, researchers have made great efforts to develop the PEMs to minimize the methanol crossover problem [16-17].

Various sulfonated polymers, including Nafion, sulfonated arylene ether sulfone, polyether ketone, and sulfonated polysulfone are utilized as polymer electrolyte membranes to overcome the problem of methanol penetration [18-22]. Because of its superior mechanical, thermal, and chemical resistance as well as its high proton conductivity, Nafion is widely utilized as a proton conductor [23-24]. However, using the Nafion membrane in DMFC has various drawbacks, such as complicated production techniques high costs, environmental unavailability, and significant methanol crossover [25-27].

Fabricated membranes with a composite material improve their performance. Many organic and inorganic materials have been used as a booster to fabricate the composite membrane, including sodium dodecylbenzene sulfonate, Graphene Oxide (GO), poly(styrenesulfonic acid) (PSSA), Carbon NanoTube (CNT), sulfonated polyimide, sulfonated polybenzimidazoles, sulfonated polysulfone and sulfonated poly (phenylene oxide), zirconia, clays, zeolites, metal-organic frameworks (MOFs) [28-34]. Among these materials, MOFs attracted considerable attention due to their interesting structure-related properties and an endless number of possible structures [35-36]. The presence of amine groups in MIL-53(Al)-NH$_2$ allows for simultaneous H$^+$ transport through the membrane, resulting in high proton conductivity [37].

Consequently, the addition of this metal-organic compound to the membrane appears to improve the membrane's performance by allowing for easy proton exchange. In this study, The SPS-PE-MIL-53 was synthesized in p-xylene at 348 K and characterized by FT-IR, SEM, and TGA. Water absorption, proton conductivity, oxidative resistance, ionic conductivity, and methanol permeability are all examined to identify the membrane's efficiency in a direct methanol fuel cell.

EXPERIMENTAL SECTION
Characterization and measurement

All materials and reagents such as dichloromethane, acetic anhydride, sulfuric acid 98 %, Al(NO$_3$)$_3$.9H$_2$O, 2-aminoterephthalic acid, N, N´-dimethylformamide, p-Xylene, and polystyrene (PS) were purchased from Merck, Germany. Linear low-density polyethylene (LDPE; density 0.92 g.cm^3, surface hardness SD48, tensile strength 20 Mpa, linear expansion $20{\times}10^{-5}$ 1/°C, water adsorption 0.01 %, volume resistivity $10^{16}\Omega$.cm and melting temperature range 120-160 °C) was purchased from Bandar Imam Petrochemistry, Iran.

Using a JASCO-460 FT-IR spectrometer, FT-IR spectra of the materials and membranes were taken. They had a spectral range between 400-4000 1/cm. Through Scanning Electron Microscopy (SEM) equipped with an SEM instrument (MIRA3 TESKAN), the surface morphology and the sample's status were studied. After cooling in the liquid nitrogen, the dry membranes were manually fractured. The samples were sputter-coated with gold (15 nm thickness). Also, they were imaged on SEM at 5kV. A thermal gravimetric analysis was conducted by a TGA/DSC 1 (TGA Q50) with a heating rate of 10 K/min in the atmosphere of N$_2$ at a flow rate of about 50 mL/min. A four-probe method was used to measure the proton conductance of the membrane by the Electrochemical Impedance Spectroscopy (EIS) with a Zahner potentiostat/galvanostat electrochemical workstation model PGSTAT over the frequency range of 4MHz-1Hz with the oscillating voltage of 5 mV.

Preparation of SPS

Sulfonated Polystyrene (SP) was prepared by the method of *Makowski et al.* [38, 39]. First, 50 mL acetyl sulfate solution 2.0 M was prepared, and mixed with an equal amount of dichloromethane and acetic anhydride under a nitrogen atmosphere and cooled to 273 K. A solution of sulfuric acid 98 % was gradually added and the mixture was stirred at room temperature until a clear homogeneous solution was obtained. Extra acetic anhydride was used to clear any trace of water.

In a round-bottomed flask, 20.0 g of PS was dissolved in 500 mL of CH$_2$Cl$_2$ for the sulfonation reaction. The flask was heated to 313 K, and cleaned with N$_2$ for 40 min, to obtain the total stability of PS. Then, a freshly prepared acetyl sulfate solution was added to the reaction mixture. The mixture was kept at 313 K while stirring for 2 hours.

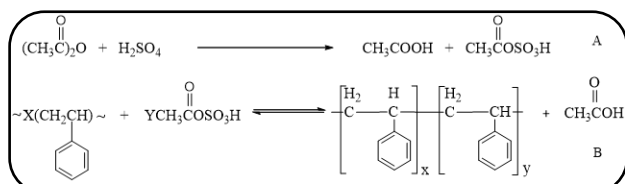| Chemical	Formula	Abbreviation
Sulfonated polystyrene	$[C_8H_7SO_3^-]_n$	SPS
Polyethylene	$(C_2H_4)_n$	PE
MIL-53(Al)-NH$_2$	$Al(OH)(O_2C–C_6H_3(NH_2)–CO_2)(H_2O)$	MIL-53
Prepared membrane	A combination of the above	SPS-PE-MIL-53

Fig. 1: Schematic reaction of A) acetylsulfate generation and B) SPS generation.

After adding the sulfonating agent, a transparent yellow solution was produced. The reaction was terminated when an excess of 2-propanol was added for 30 minutes and cooled at room temperature. Ultimately SPS was isolated and dried at 303 K for 24 h in a vacuum oven. A schematic of the two-step SPS production is shown in Fig 1.

Synthesis of MIL-53(Al)-NH$_2$

MIL-53(Al)–NH$_2$, was prepared as described elsewhere [37]. 2.0 g of Al(NO$_3$)$_3$.9H$_2$O, 1.0 g of 2-aminoterephthalic acid, and 15 mL of water were added to 100 mL Teflon-lined steel autoclave. The autoclave was heated for 5 hours in an oven at 423 K. The solution was filtered, and the compound was refluxed in N, N´-dimethylformamide at 423 K for 12 hours, and then it was dried for one day in an oven at 423 K. A yellow powder of MIL-53(Al)–NH$_2$ was obtained.

Preparation of SPS-PE-MIL-53 membrane

1.0 g of LDPE was first dissolved in 30 mL p-xylene, then it was stirred at 300 rpm for 2 hours and 373 K, to form a homogeneous solution. Also, 1.0 g of SPS with (0.1, 0.25, 0.5) g of MIL-53(Al)–NH$_2$ was added, mixed, and dissolved in p-xylene to provide a yellow polymer solution. The solutions were poured onto the glass plates, and they were dried at 318 K for 24 hours, and then at 348 K in a vacuum for 12 hours. The membrane was peeled off and designated as SPS-PE-MIL-53. Before using this PEM "SPS-PE-MIL-53" in direct methanol fuel cell, it was transformed to the H$^+$ through boiling it first in the deionized water for half-hour and then in 1.0 M H$_2$SO$_4$ for 24 hours. After that, extra

H$_2$SO$_4$ was removed by rinsing and boiling in the deionized water. Table 1 shows the chemicals used in the preparation of the membrane and their abbreviations.

Evaluating the properties of the membrane

To recognize the improved overall performance of the prepared membranes, various properties, including the water uptake rate, ion exchange capacity, methanol permeability, and selectivity, had significant influences, and they should be measured.

The water uptake was calculated to measure the membrane's water retention capability. It was determined by measuring the weight change before and after hydration. The membrane was immersed in the Double-Distilled Water (DDW) for 24 hours for surface saturation, resulting alignment of water molecules in response to the charge which is an important factor affecting membrane transport and and reactivity.

After removing the surface water, the membrane was weighted quickly to determine the wetted membrane weight (W_w). The dry membrane weight (w_d) was determined when the membrane was dried at 373 k for 2 hours. Eq. (1) was used for calculating the water uptake [40]:

$$Water\ uptake\ (\%) = \frac{Ww - Wd}{Wd} \times 100 \qquad (1)$$

The back-titration method determined the ion exchange capacity (IEC). The sample was dried until the weight was constant, then the sample was immersed in 50 mL of saturated NaCl for 24 hours to release the H$^+$ ions into the solution using the ion-exchange reaction with Na$^+$ ions. Using phenolphthalein as an indicator, the ion-exchanged solution was titrated with 0.01 M NaOH. The IEC was calculated by Eq. (2) [22]:

$$IEC = \frac{V_{NaOH} \times C_{NaOH}}{W_{dry}} \qquad (2)$$

In this equation, W_{dry} (g) is the membrane's dry mass, V_{NaOH} (L) is the volume of the titrated NaOH solution, and C_{NaOH} (mol/L) is the NaOH's molar concentration in the solution.

A piece of the membrane was immersed into the Fenton's reagent under stirring (3% H$_2$O$_2$ aqueous solution with 2 ppm FeSO$_4$) for 1 hour at 80 °C to examine the membrane resistance to the free radical species. The oxidative durability was assessed by measuring the time necessary to completely dissolve and maintaining the membrane weight after 2 hours in the reagent.
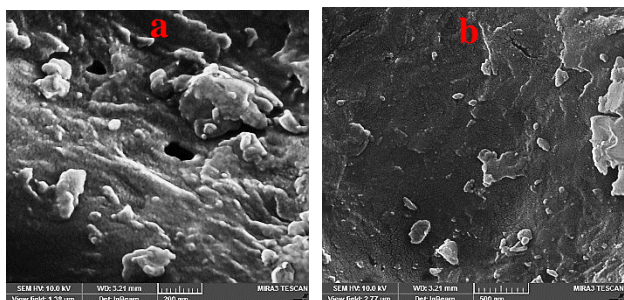
Fig. 2: SEM image for (a) MIL-53(Al)-NH₂ (b) SPS-PE-MIL-53(Al)-NH₂ membrane.

The proton conductance of the membrane was measured through a four-probe method [41] by EIS with a Zahner potentiostat/galvanostat electrochemical workstation model (PGSTAT) over a frequency range of 4MHz-1Hz with the oscillating voltage of 5 mV. Two inner platinum (Pt) wires (with 0.2 mm diameter) serving as voltage sensors and Two outer platinum (Pt) wires (with 0.2 mm diameter) serving as AC injectors were used for this four-probe method. The membrane sample (size of ca. 3×1.0 cm²) was squeezed between the two Teflon blocks and it was held in its place using the nylon screws. In order to be activated, the membranes were soaked in a 1.0 M HCl solution for 12 hours, before this test. After that, they were washed using deionized water until their pH became 7. The proton conductance was measured within the temperature range of 30 °C in the liquid water. Eq. (3) was used to calculate the proton conductance from the impedance data [41]:

$$\sigma = \frac{L}{RWd} \tag{3}$$

In the Equation (3), σ is the proton conductance (S/cm), L is the distance between potential-sensing electrodes (cm), R is the resistance associated with the ionic conductance of a membrane from the impedance data (Ω), W is the width of the membrane (cm), and d is the thickness of the membrane (cm).

The permeability of methanol through the membrane was measured by a two-compartment diffusion cell. The membrane between the two glass compartments was vertically clamped, and each one contained a magnetic stirring bar to agitate the solution. The feed part was filled with 5.0 M methanol, and the receiving one was filled with deionized water. Also, the concentration of the methanol within the receiving compartment was evaluated. Besides, the membrane permeability was calculated using the Equation (4) [41-42]:

$$P = \frac{1}{CA}\left(\frac{\Delta C_{B(t)}}{\Delta t}\right)\left(\frac{LV_B}{A}\right) \tag{4}$$

In the Eq. (4), P is the methanol diffusion permeability of the membrane (cm²/s), C_A is the methanol concentration in the cell A (mol/L), $\Delta C_{B(t)}/\Delta t$ is the slope of the molar concentration variation of methanol in the cell B as a function of time (mol/L.s), V_B is the volume of each diffusion reservoir (cm³), A is the membrane area (cm²), and L is the thickness of membrane (cm).

At last, the selectivity factor (the ratio of proton conductance to the methanol permeability) was determined using the equation below [41, 42]:

$$\text{Selectivity} = \frac{\sigma}{P} \tag{5}$$

RESULT AND DISCUSSION
SEM characterization

The membranes' structure and morphology were characterized using SEM measurements. The SEM micrographs of MIL-53 and SPS-PE-MIL-53 membranes have been depicted in Fig. 2. The SEM image of particles of MIL-53 has been shown in Fig. 2a. The surface of MIL-53 particles is porous without any agglomeration. The porosity of the metal-organic framework (MIL-53) leads to incorporating more functional groups into the network, and these functional groups (COOH) and (NH₂) will facilitate the better transfer of protons through the membrane. Fig. 2b shows that the hybrid SPS-PE-MIL-53 with a uniform matrix membrane has a dense structure, whereas the presence of the fine micrograph parts on the membrane surface, which could be observed in the SEM image, confirms the presence of SO₃⁻, COOH, and NH₂ groups in the SPS-PE-MIL-53 membranes. The dense homogeneous surface of the prepared membranes could be ascribed to the harmony between the polymer and the particle that provides a simple pathway for proton conduction through the ionic channels present in the polymer matrix.

The characterization of FT-IR
In the previous work, we explained the FT–IR key bands of the PE and SPS [40-42]. Fig. 3. shows the FT-IR spectrum for MIL-53 and SPS-PE-MIL-53. Fig. 3 (a) presents the FT-IR curve for MIL-53. The centralization of the very strong bands at 3421 1/cm, which could be due to the functional groups of the COOH and NH₂ has been clearly depicted in the figure. The width of this peak
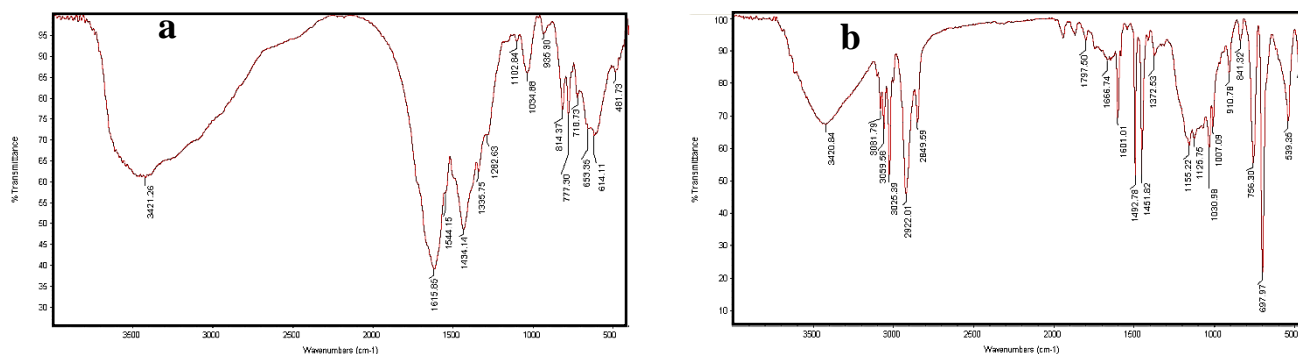
Fig. 3: FT-IR image for (a) MIL-53 and (b) SPS-PE-MIL-53.

implies that these functional groups are abundant on the MIL-53 structure. These groups can create hydrogen bonds with water, and absorb some water. The amount of water content of the membrane in a DMFC is very important because it is directly related to the amount of proton conduction by the membrane. The strong bands at 1615 1/cm are due to the C=O stretching of COOH groups, whereas the bands at 1434 1/cm are due to the O–H deformation of C–OH groups. Fig. 3 (b) indicates the FT-IR curve for the SPS-PE-MIL-53 membrane. The figure clearly shows that the centralization of the strong bands at 3420 1/cm could be due to the functional groups of COOH and NH_2. Given the low amount of the MIL-53 in the membrane fabrication, this bond is weaker than the same band in Fig. 3 (a). The aliphatic C-H stretching absorbance of methylene and methylene groups in the main chain leads to the bands at 2849-3081 1/cm. At 1372 1/cm, SO_2 asymmetric stretching occurs. The bands at 1797 1/cm appear because of the C=O stretching of COOH groups, and the bands at 1451 and 1492 1/cm appear because of the O–H deformation of C–OH groups. The four peaks at 1007 1/cm, 1030 1/cm, 1125 1/cm, 1155 1/cm could be attributed to the symmetric stretching of SO_3.

Water uptake

The fuel cell membranes could transfer protons from the anode side to the cathode side of the membrane. Therefore, the higher the water absorption by the membrane is, the better the transfer of protons would be from the anode side to the cathode side. However, the role of the water absorbed by the membrane is like a double-edged sword because the water absorbed by the membrane can swell the membrane and undermine its mechanical properties. Fig. 4 shows the water content of the prepared composite membranes, which were equilibrated with 100%
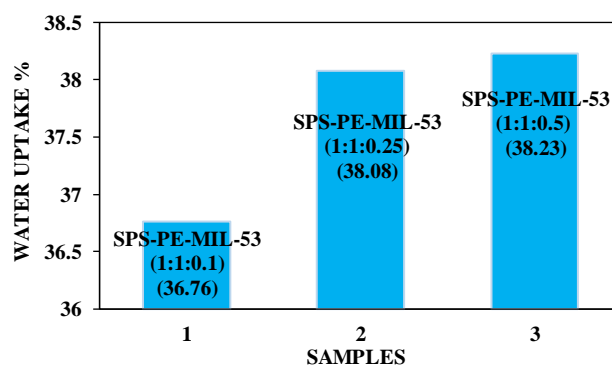

Fig. 4: Water uptake of the composite membranes

air relative humidity at 25 °C. Also, it was immersed in liquid water at the same temperature. As it has been shown in Fig. 4, the order of the membranes' water content is as SPS-PE-MIL-53 (1:1:0.5 w:w:w) > SPS-PE-MIL-53 (1:1:0.25 w:w:w) > SPS-PE-MIL-53 (1:1:0.1 w:w:w). This indicates that the more MOF content, the more water is absorbed. However, the amount of water absorbed by the SPS-PE-MIL-53 (1:1:0.5) membrane is very close to that of the SPS-PE-MIL-53 (1:1:0.25) membrane. Functional groups in the MOF structure, such as the COOH and NH_2 groups, could help the membrane absorb more water because of the hydrogen bonding they could form with water.

Proton conductivity

One of the main properties of the membranes used by DMFCs is their ability to easily transfer the protons from the anode side to the cathode side. Different functional groups could be applied to the prepared membranes to facilitate proton transfer. Operative groups such as sulfonic acid, amine, and carboxylic acid are the three important groups that can be utilized for this purpose. In the present study, all three functional groups have been used. These functional groups help absorb more water in
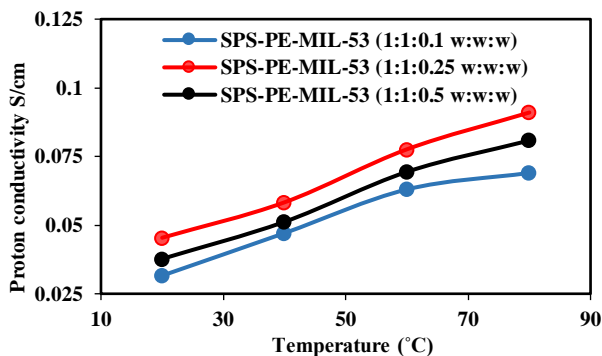
Fig. 5: Proton conductance of composite membranes.

the membrane by forming hydrogen bonds with the water molecules. More water absorption by the membrane would lead to better proton transfer through the membrane. Proton conductance is also expected to increase with the increment of MIL-53 in the prepared membranes. Different proton conductance of the membranes at different temperatures has been depicted in Fig. 5. The figure clearly shows that the proton conductance increases by enhancing the temperature from 20 ° C to 80 ° C. Also, as it has been demonstrated in Fig. 5, when the amount of MIL-53 which was used in the membranes' preparation increased from 0.1 g to 0.25 g, the proton conductance increased as well. This could be due to the increasing number of COOH and NH_2 functional groups inside the membrane. However, the proton conductance decreased when the value was increased from 0.25 g to 0.5 g. The increase in MIL-53 in the membranes from a certain amount further increases the resistance to the proton mass transmission through the membrane, which may be due to the bonds formed between the COOH and NH_2 functional groups in the MIL-53 and the polystyrene sulfonic groups. However, the optimum value of 0.25 g of the MIL-53 for the preparation of the membrane was chosen in this work.

Methanol permeability, selectivity factor, ion exchange capacity, and oxidative stability

Table 2 summarizes the IEC, proton conductance, methanol permeability, selectivity, and oxidative stability of the composite membranes. The IEC displays the membrane's ability for proton transmission from the anodic to the cathodic side in DMFC. It is an appropriate parameter for determining the aggregation of proton exchangeable groups and also the proton conductance of the membranes. According to the experiment, we measured the IEC for the prepared membranes. We measured

the IEC for the prepared membranes. The IEC measurements revealed that all of the composite membranes had high IEC values, indicating that the membranes have good proton transferability.

We estimated the conductance of the protons by the membrane samples at 20 °C and a relative humidity of 100%. Moreover, we performed the composite membranes' test with water for one day. Table 2 shows that the composite membranes had good proton conductivity [43]. By a 5.0 M solution of methanol, we measured the permeability of methanol of the membrane samples at room temperature. The permeability values of methanol in the composite membranes have been shown in Table 2. The results of the measurements of the permeability of methanol indicate that the order of the permeability of methanol in the synthesized membranes is as follows: SPS-PE-MIL-53 (1:1:0.5 w:w:w) > SPS-PE-MIL-53 (1:1:0.25 w:w:w) > SPS-PE-MIL-53 (1:1:0.1 w:w:w). It means that by increasing the amount of MIL-53 in the membranes, the permeability of methanol increases; however, the values of methanol permeability are very close to each other. A low methanol permeability membrane is beneficial for DMFC use. Since the DMFC membranes' goal is to enhance the conductance of protons and decrease the permeability of methanol, the selectivity factor (the ratio of the conductance of protons and the permeability of methanol) can be used as a guide to developing better DMFC properties. The higher selectivity factor leads to better performance of DMFC. The results of the selectivity factor have been presented in Table 2.
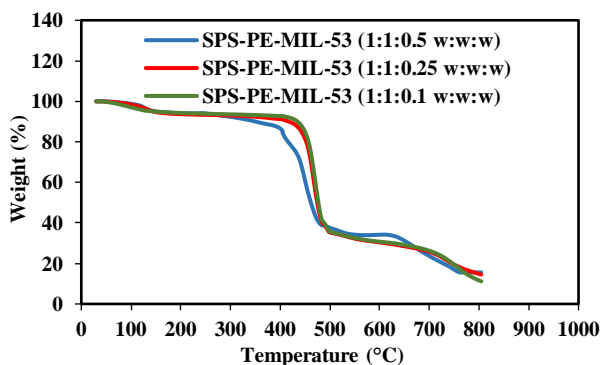
Also, the research results on the oxidation stability of the composite membranes were tested in Fenton's reagent at 80 °C (Table 2). As the results show, these membranes had good stability, as more than 98% of their weight was retained after 1 hour. The great performance of the membrane in terms of oxidative stability could be attributed to the cross-linking network which was developed between the SPS-PE and the metal-organic functional group framework (MIL-53).

TGA characterizations

Fig. 6 shows TGA curves for the membranes which were produced by the SPS-PE-MIL-53. All three synthesized membranes showed excellent thermal resistance that was very close to each other (see Fig. 6). However, the membranes' thermal resistance reduced slightly as the amount of MIL-53 added to the membranes

Table 2: IEC, proton conductance, the permeability of methanol, selectivity, and oxidative stability factor of the composite membranes
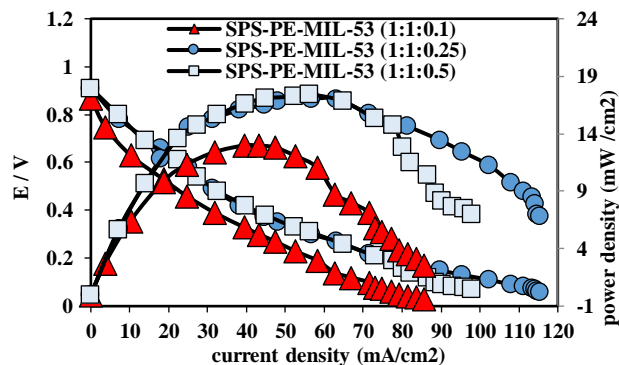
Membrane	IEC (meq/g)	Proton conductivity (S/cm)	Methanol permeability (cm²/s)	Selectivity factor (S.s/cm³)	Oxidative stability (Wt %)
SPS-PE-MIL-53 (1:1:0.1 w:w:w)	0.95	3.16×10^{-2}	5.96×10^{-7}	5.30×10^{4}	> 98
SPS-PE-MIL-53 (1:1:0.25 w:w:w)	0.97	4.54×10^{-2}	6.33×10^{-7}	7.17×10^{4}	> 98
SPS-PE-MIL-53 (1:1:0.5 w:w:w)	0.97	3.77×10^{-2}	6.61×10^{-7}	5.70×10^{4}	> 98

Fig. 6: TGA analysis of the membranes within a range of 30 to 800 °C.

Fig. 7: Current density potential (I-V) and the power density curves of the DMFC gathered with different produced membranes at 80 ºC.

increased. The parameters related to this weight-loss area degraded in four weight zones for all membranes. The first weight-loss zone occurred around 85–140 °C. Because membranes are known to absorb a lot of water, the weight loss might be due to the loss of the absorbed water. The next major weight-loss zone occurred around 360-500 °C. In this zone, there are weight losses of 60-70%. The highest mass loss accompanied this observed zone of weight loss. Therefore, it was called the main stage. As a result, this mass loss could be attributed to the full thermal degradation of the composite's skeletal chain structure. Weight loss over 600 °C for SPS-PE-MIL-53 membranes could be used for the organic moieties removal. The decomposition of MIL-53 and polystyrene leads to weight loss within the temperature range of 700–800 °C.

The performances of single-cell

Single-cell tests for the composite membranes for CH_3OH/O_2 were performed to understand the proposed membrane performance. The performance of the proposed system relies on the membrane's composition, the electrochemical reaction efficiency at the interface between the solid phases of electrodes and the liquid and gas phases in the anode and cathode sides, the temperature of the fuel cell, the flow rate, and the concentration of methanol in the carrier stream. Fig.7 illustrates the findings of single-cell testing with MEAs produced by

SPS-PE-MIL-53 (1:1:0.5 w:w:w), SPS-PE-MIL-53 (1:1:0.25 w:w:w), and SPS-PE-MIL-53 (1:1:0.1 w:w:w) inside Oxygen in the cathode side and the aqueous solution of 2.0 M methanol in the anode side at 80 ºC with 1.0 mL/min flow rate. As it could be observed, the DMFC based on SPS-PE-MIL-53 (1:1:0.25 w:w:w) membrane has a maximum peak power density of 17.04 mW/cm², with a maximum current density of 115.38 mA/cm²; while the DMFC equipped with the SPS-PE-MIL-53 (1:1:0.5 w:w:w) membrane has a maximum peak power density of 17.41 mW/cm² with a maximum current density of 97.86 mA/cm² and the DMFC equipped with the SPS-PE-MIL-53 (1:1:0.1 w:w:w) membrane has a maximum peak power density of 12.97 mW/cm² with a maximum current density of 85.50 mA/cm². Because of the increased selectivity in the produced membranes, the proton exchange and the permeability of methanol through the membranes in DMFCs directly influence the OCV. It was found that the OCV in SPS-PE-MIL-53 (1:1:0.25 w:w:w) membrane (0.91V) is higher than SPS-PE-MIL-53 (1:1:0.1 w:w:w), and it is similar to SPS-PE-MIL-53 (1:1:0.5 w:w:w).

CONCLUSIONS

We successfully incorporated MIL-53(Al)-NH₂ particles into the membranes through casting, and prepared the composite membranes. In this work, different amounts of

MIL-53(Al)-NH$_2$ (0.1, 0.25, and 0.5 g) were used to prepare the membranes. Various parameters such as proton conductance, water uptake, and methanol permeability were studied for the different membranes. The SPS-PE-MIL-53 (1:1:0.5 w:w:w) membrane had more water uptake than the other two membranes. The proton conductance in the SPS-PE-MIL-53 (1:1:0.25 w:w:w) membrane was higher than the other membranes. SPS-PE-MIL-53 (1:1:0.25 w:w:w) membrane also showed good resistance to the permeability of methanol compared to the other membranes. Thermal resistance was evaluated by examining the TGA diagram, which showed that all prepared membranes had proper thermal resistance. The fuel cell performance test was conducted for the prepared membranes, and the synthesized membranes worked well. The SPS-PE-MIL-53 (1:1:0.25 w:w:w) membrane showed relatively better performance than the other membranes.

Acknowledgments

REFERENCES

[1] Shukla A., Dhanasekaran P., Sasikala S., Nagaraju N., Bhat S.D., Pillai V.K., Covalent Grafting of Polystyrene Sulfonic Acid on Graphene Oxide Nanoplatelets to form a Composite Membrane Electrolyte with Sulfonated Poly (Ether Ether Ketone) for Direct Methanol Fuel Cells, *J. Membr. Sci.*, **595:** 117484 (2020).

[2] Shukla A., Dhanasekaran P., Sasikala S., Nagaraju N., Bhat S.D., Pillai V.K., Nanocomposite Membrane Electrolyte of Polyaminobenzene Sulfonic Acid Grafted Single Walled Carbon Nanotubes with Sulfonated Polyether Ether Ketone for Direct Methanol Fuel Cell, *Int. J. Hydrog. Energy.*, **44(50):** 27564-27574 (2019).

[3] Naeimi, A., Ekrami-Kakhki, M.S., Donyagard, F. Enhanced Electrocatalytic Performance of Pt Nanoparticles Immobilized on Novel Electrospun PVA@ Ni/NiO/Cu Complex Bio-Nanofiber/Chitosan based on Calotropis Procera Plant for methanol electro-Oxidation, *Int. J. Hydrog. Energy.*, **46(36):** 18949-18963 (2021).

[4] Wang Y, Ruiz Diaz D.F, Chen K. S, Wang Z, Adroher X.C. Materials, Technological Status, and Fundamentals of PEM Fuel Cells - A Review, *Mater Today.*, **32:** 178-203 (2020).

[5] Khammarnia S., Akbari A., Ekrami-Kakhki M.S., Saffari J. Enhanced Catalytic Activity of Pt-NdFeO$_3$ Nanoparticles Supported on Polyaniline-Chitosan Composite Towards Methanol Electro-Oxidation Reaction, *J Nanostruct,* **10(2):** 239-257 (2020).

[6] Ekrami-Kakhki M.S., Naeimi A., Donyagard F., Pt Nanoparticles Supported on a Novel Electrospun Polyvinyl Alcohol-CuOCo$_3$O$_4$/Chitosan based on Sesbania Sesban Plant as an Electrocatalyst for Direct Methanol Fuel Cells, *Int. J. Hydrog. Energy.*, **44(3):** 1671-1685 (2019).

[7] Ahn C.Y., Ahn J., Kang S.Y., Kim O.H., Lee D.W., Lee J.H., Goo Sh. J, Chang Hyun L, Cho Y-H, Sung Y.E., Enhancement of Service Life of Polymer Electrolyte Fuel Cells through Application of Nanodispersed Ionomer, *Science advances.*, **6:** 1-9 (2020).

[8] Ekrami-Kakhki M.S., Farzaneh N., Abbasi S., Makiabadi B. Electrocatalytic Activity of Pt Nanoparticles Supported on Novel Functionalized Reduced Graphene Oxide-Chitosan for Methanol Electrooxidation, *J. Mater. Sci.: Mater. Electron., 28*(**17**)**:** 12373-12382 (2017).

[9] Kang K., Park S., Cho S.O., Choi K., Ju H., Development of Lightweight 200-W Direct Methanol Fuel Cell System for Unmanned Aerial Vehicle Applications and Flight Demonstration, *Fuel cells.* **14(5):** 694-700 (2014).

[10] Rasheed, R.K.A., Liao, Q., Caizhi, Z., Chan, S.H., A Review on Modelling of High Temperature Proton Exchange Membrane Fuel Cells (HT-PEMFCs), *Int. J. Hydrog. Energy*, **42(5):** 3142-3165 (2017).

[11] Cai W., Fan K., Li J., Ma L., Xu G., Xu S., Ma L., Cheng H., A Bi-Functional Polymeric Nano-Sieve Nafion Composite Membrane: Improved Performance for Direct Methanol Fuel Cell Applications, *Int. J. Hydrog. Energy.*, **41(38):** 17102- 17111 (2016).

[12] Müller M., Kimiaie N., Glüsen A., Direct Methanol Fuel Cell Systems for Backup Power–Influence of the Standby Procedure on the Lifetime, *Int. J. Hydrog. Energy*, **39(36):** 21739-21745 (2014).

[13] Escudero-Cid R., Montiel M., Sotomayor L., Loureiro B., Fatás E., Ocón P., Evaluation of Polyaniline-Nafion® Composite Membranes for Direct Methanol Fuel Cells Durability Tests, *Int. J. Hydrog. Energy*., **40(25):** 8182 (2015).

[14] Nasiri M., Atabaki F., Ghaemi N., Seyedzadeh Z., Fabrication and Characterization of Proton Conductive Membranes Based on Poly(methyl methacrylate-co-maleic anhydride), *Iran. J. Chem. Chem. Eng. (IJCCE),* **39(1):** 43-57 (2020).

[15] Lee S., Choi B.G., Choi D., Park H.S., Nanoindentation of Annealed Naf Ion/Sulfonated Graphene Oxide Nanocomposite Membranes for the Measurement of Mechanical Properties, *J. Membr. Sci.* **451:** 40-45 (2014).

[16] Rambabu G., Bhat S.D., Sulfonated Fullerene in SPEEK Matrix and its Impact on the Membrane Electrolyte Properties in Direct Methanol Fuel Cells, *Electrochim. Acta*, **176:** 657-669 (2015).

[17] Yuan T., Pu L., Huang Q., Zhang H., Li X., Yang H., An Effective Methanol-Blocking Membrane Modified with Graphene Oxide Nanosheets for Passive Direct Methanol Fuel Cells, *Electrochim. Acta,* **117:** 393-397 (2014).

[18] Kim D.J., Hwang H.Y., Jung S.B., Nam S.Y., Sulfonated Poly (Arylene Ether Sulfone)/Laponite-SO_3H Composite Membrane for Direct Methanol Fuel Cell, *J. Ind. Eng. Chem*., **18(1):** 556-562 (2012).

[19] Li C., Sun G., Ren S., Liu J., Wang Q., Wu Z., Sun H. Jin W., Casting Nafion–Sulfonated Organosilica Nano-Composite Membranes used in Direct Methanol Fuel Cells, *J. Membr. Sci.*, **272(1-2):** 50-57 (2006).

[20] Elumalai V., Sravanthi C.K.K., Sangeetha D., Synthesis Characterization and Performance Evaluation of Tungstic Acid Functionalized SBA-15/SPEEK Composite Membrane for Proton Exchange Membrane Fuel Cell, *Appl. Nanosci.*, **9:** 1163-1172 (2019).

[21] Luo Q., Zhang H., Chen J., You D., Sun C., Zhang Y., Preparation and Characterization of Nafion/SPEEK Layered Composite Membrane and its Application in Vanadium Redox Flow Battery, *J. Membr. Sci.,* **325(2):** 553-558 (2008)

[22] Li C., Xiao L., Jiang Z., Tian X., Luo L., Liu W., Xu Z.L., Yang H., Jiang Z.J., Sulfonic Acid Functionalized Graphene Oxide Paper Sandwiched in Sulfonated Poly (Ether Ether Ketone): A Proton Exchange Membrane with High Performance for Semi-Passive Direct Methanol Fuel Cells, *Int. J. Hydrog. Energy*, **42(26):** 16731-16740 (2017).

[23] Yen C.Y., Lee C.H., Lin Y.F., Lin H.L., Hsiao Y.H., Liao S.H., Chuang C.Y., Ma C.C.M., Sol–Gel Derived Sulfonated-Silica/Nafion® Composite Membrane For Direct Methanol Fuel Cell, *J. Power Sources.*, **173(1):** 36-44 (2007)

[24] Prapainainar P., Maliwan S., Sarakham K., Du Z., Prapainainar C., Holmes S.M., Kongkachuichay P., Homogeneous Polymer/Filler Composite Membrane by Spraying Method for Enhanced Direct Methanol Fuel Cell Performance, *Int. J. Hydrog. Energy*, **43(31):** 14675-14690 (2018).

[25] Hasanabadi, N., Ghaffarian, S. R., Hasani-Sadrabadi, M.M., Magnetic Field Aligned Nanocomposite Proton Exchange Membranes based on Sulfonated Poly (Ether Sulfone) and Fe_2O_3 Nanoparticles for Direct Methanol Fuel Cell Application, *Int. J. Hydrog. Energy*., **36(23):** 15323-15332 (2011).

[26] Feng M., Meng, F., Pu Z., Jia K., Liu X., Introducing Magnetic-Responsive CNT/Fe_3O_4 Composites to Enhance the Mechanical Properties of Sulfonated Poly (Arylene Ether Nitrile) Proton-Exchange Membranes, *J. Polym. Res*., **22(3):** 1-9 (2015).

[27] Ranjani M., Pannipara M., Al-Sehemi A. G., Vignesh A., Chitosan/Sulfonated Graphene Oxide/Silica Nanocomposite Membranes for Direct Methanol Fuel Cells, *Solid State Ion.*, **338:** 153-160 (2019).

[28] Wang S., Luo H., Li X., Shi L., Cheng B., Zhuang X., Li Z., Amino Acid-Functionalized Metal Organic Framework with Excellent Proton Conductivity for Proton Exchange Membranes, *Int J Hydrogen Energy*, **46:** 1163-1173(2021).

[29] Tsai J.C., Cheng H.P., Kuo J.F., Huang Y.H., Chen C.Y., Blended Nafion®/SPEEK Direct Methanol Fuel Cell Membranes for Reduced Methanol Permeability, *J. Power Sources*, **189(2):** 958-965 (2009).

[30] Sasikala S., Meenakshi S., Bhat S.D., Sahu A.K., Functionalized Bentonite Clay-sPEEK Based Composite Membranes for Direct Methanol Fuel Cells, *Electrochim. Acta*, **135:** 232-241 (2014).

[31] Batalha J.A.F.L., Dahmouche K., Sampaio R.B., de Souza Gomes A., Structure and Properties of New sPEEK/Zirconia/Protic Ionic Liquid Membranes for Fuel Cell Application, *Macromol Mater Eng.*, **302:** 1600301 (2017).

[32] Ponce M.L., Prado L.A.S.A., Ruffmann B., Richau K., Mohr R., Nunes S.P., Reduction of Methanol Permeability in Polyetherketone–Heteropolyacid Membranes, *J. Membr. Sci.*, **217:** 5-15 (2003).

[33 Venkatesan P.N., Dharmalingam S., Effect of Zeolite on SPEEK/Zeolite Hybrid Membrane as Electrolyte for Microbial Fuel Cell Applications, *RSC Adv.*, **5:** 84004-84013 (2015).

[34] Beydaghi H., Javanbakht M., Bagheri A., Salarizadeh P., Ghafarian-Zahmatkesh H., Kashefi S., Kowsari E., Novel Nanocomposite Membranes Based on Blended Sulfonated Poly (Ether Ether Ketone)/Poly (Vinyl Alcohol) Containing Sulfonated Graphene Oxide/Fe$_3$O$_4$ Nanosheets for DMFC Applications, *RSC Adv.*, **5:** 74054-74064 (2015).

[35] Yaghi O.M., O'Keeffe M., Ockwig N.W., Chae H.K., Eddaoudi M., Kim J., Reticular Synthesis and the Design of New Materials, *Nature.*, **423:** 705-714 (2003).

[36] Li J.R., Sculley J., Zhou H.C., Metal–Organic Frameworks for Separations, *Chem. Rev.*, **112:** 869-932 (2012).

[37] Shigematsu A., Yamada T., Kitagawa H., Wide Control of Proton Conductivity in Porous Coordination Polymers, *J. Am. Chem. Soc.*, **133(7):** 2034-2036 (2011).

[38] Makowski H.S., Lundberg R.D., Singhal G.H., EXXON Research and Engineering Company, *US pat.*, **19(2):** 310 (1975).

[39] Martins C.R., Ruggeri G., De Paoli M.A., Synthesis in Pilot Plant Scale and physical Properties of Sulfonated Polystyrene, *J. Braz Chem. Soc.*, **14:** 797-802 (2003).

[40] Mandanipour V., Noroozifar M., Modarresi-Alam A.R., Preparation of Modified Sulfonated Poly (Styrene Divinylbenzene) with Polyaniline as a New Polymer Electrolyte Membrane for Direct Methanol Fuel Cell, *Int. J. Electrochem.*, **11:** 5302-5317 (2016).

[41] Mandanipour V., Noroozifar M., Modarresi-Alam A.R., Khorasani-Motlagh M., Fabrication and Characterization of a Conductive Proton Exchange Membrane based on Sulfonated Polystyrenedivinylbenzene Resin-Polyethylene (SPSDR-PE): Application in Direct Methanol Fuel Cells, *Iran. J. Chem. Chem. Eng.*, **36:** 151-162 (2017).

[42] Mandanipour V., Chemical Modification of Proton Exchanger Sulfonated Polystyrene with Sulfonated Graphene Oxide for Application as A New Polymer Electrolyte Membrane in Direct Methanol Fuel Cell, *Iran. J. Chem. Chem. Eng. (IJCCE)*, **40(6):** 1973-1984 (2021).

[43] Li Y., Hoorfar M., Shen K., Fang J., Yue X., Jiang Z., Development of a Crosslinked Pore-Filling Membrane with an Extremely Low Swelling Ratio and Methanol Crossover for Direct Methanol Fuel Cells, *Electrochim. Acta*, **232:** 226-235 (2017).